BBA - Biomembranes 1863 (2021) 183471

Contents lists available at ScienceDirect

BBA - Biomembranes

journal homepage: www.elsevier.com/locate/bbamem

Mitochondria membrane transformations in colon and prostate cancer and their biological implications

Shani Ben Zichri[a], Sofiya Kolusheva[b], Alexander I. Shames[c], Elina Abaev Schneiderman[d], Juan L. Poggio[e], David E. Stein[e], Elena Doubijensky[b], Dan Levy[d], Zulfiya Orynbayeva[e,*], Raz Jelinek[a,b,**]

[a] Department of Chemistry, Ben-Gurion University, Beer-Sheva 84105, Israel
[b] Ilze Katz Center for Nanotechnology, Ben-Gurion University, Beer-Sheva 84105, Israel
[c] Department of Physics, Ben-Gurion University, Beer-Sheva 84105, Israel
[d] Department of Microbiology, Immunology and Genetics, Faculty for Health Sciences, Ben-Gurion University, Beer-Sheva 84105, Israel
[e] Department of Surgery, Drexel University College of Medicine, Philadelphia, PA 19102, USA

ARTICLE INFO

Keywords:
Prostate cancer
Colon cancer
Mitochondrial membrane
Submitochondrial particles (SMPs)
Cardiolipin
Betulinic acid
Resveratrol

ABSTRACT

Mitochondria have emerged as important determinants in cancer progression and malignancy. However, the role of mitochondrial membranes in cancer onset and progression has not been thoroughly investigated. This study compares the structural and functional properties of mitochondrial membranes in prostate and colon cancer cells in comparison to normal mitochondria, and possible therapeutic implications of these membrane changes. Specifically, isolation of cell mitochondria and preparation of inverted sub-mitochondrial particles (SMPs) illuminated significant cancer-induced modulations of membrane lipid compositions, fluidity, and activity of cytochrome *c* oxidase, one of the key mitochondrial enzymes. The experimental data further show that cancer-associated membrane transformations may account for mitochondria targeting by betulinic acid and resveratrol, known anti-cancer molecules. Overall, this study probes the relationship between cancer and mitochondrial membrane transformations, underlying a potential therapeutic significance for mitochondrial membrane targeting in cancer.

1. Introduction

Cancer is a complex disease, characterized by reprogrammed signaling, changes in cell physiology and uncontrolled cell growth. Prostate and colon cancers are the most prevalent cancers worldwide among men [1]. The morbidity and mortality rates of prostate cancer rise with age, while there has been increasing mortality from colorectal cancer among people younger than 50 [2]. Despite the high rate of incidence, effective means to cure these cancers are still limited [3]. Early stage surgical and chemotherapeutic interventions help block the disease, however once a tumor metastasizes these cancers become incurable.

Malignant tumors are characterized by high proliferation rates and concomitant increased energy metabolism. While elevated glycolysis is an established hallmark of energy production in cancer, the role of mitochondria in affecting the energy balance of cancer cells is believed to play an important role. Indeed, the occurrence of cancer-induced mitochondria alterations has been established in many studies. Specifically, transformations of cancer cells have been linked to mutations of mitochondrial DNA affecting activity of respiratory proteins [4] and anti-apoptotic proteins [5], changes in mitochondria membrane potential [6], and generation of reactive oxygen species [7,8]. Other cancer-associated changes in the metabolic and signaling functionalities of mitochondria have been also reported [9,10]. Mitochondria and mitochondrial proteins constitute important cancer markers and anti-cancer drug targets [11,12].

Many studies indicate significant changes in lipogenesis and cell membrane lipid organization during malignant transformations

Abbreviations: SMPs, submitochondrial particles; HCT116, human colon cancer cell line; PC-3, human prostate cancer cell line; PrEC, human prostate epithelial cells; CCD-18Co, human colon fibroblasts cell line; CL, cardiolipin; LC-MS, liquid chromatography mass spectrometry; TEM, transmission electron microscopy; COX, cytochrome *c* oxidase; EPR, electron paramagnetic resonance; 10-doxyl., 10-doxyl nonadecane

* Correspondence to: Z. Orynbayeva, Drexel University College of Medicine, 245 N 15th street, Philadelphia, PA 19102, USA.
** Correspondence to: R. Jelinek, Ben-Gurion University, Beer-Sheva 84105, Israel.
E-mail addresses: zo25@drexel.edu (Z. Orynbayeva), razj@bgu.ac.il (R. Jelinek).

https://doi.org/10.1016/j.bbamem.2020.183471
Received 18 May 2020; Received in revised form 31 August 2020; Accepted 2 September 2020
Available online 12 September 2020
0005-2736/ © 2020 Published by Elsevier B.V.

[13–15]. Specifically, cancer conditions have been correlated with changes in membrane lipid compositions [16], modulation of membrane biophysical properties such as bilayer fluidity [17] and surface charge [18], lipid asymmetry [19] and membrane dynamics [20]. Notably, much fewer studies have focused on cancer-associated changes in *mitochondrial* membranes. Higher rigidity of mitochondrial membranes isolated from hepatoma cells has been reported, ascribed to changes in lipid compositions and acyl chain saturation [21,22]. Specifically, previous studies indicated enrichment of phosphatidylethanolamine (PE) and cholesterol, modulations of cardiolipin (CL) content, and increase in the level of monounsaturated fatty acids [23–25]. Lower saturation of lipid acyl chains is a characteristic feature of tumor cells in general [22,26,27]. Mitochondrial membrane transformations are believed to favor cancer cell escape from apoptosis and developing the resistance to chemotherapy [28]. There appears, however, a significant tumor tissue-dependent variability in mitochondrial membrane properties [29].

This study examines transformations of mitochondrial membrane properties occurring in colon and prostate cancers. Recent studies reported elevated mass of mitochondria isolated from prostate and colon tumors, likely accounting for the increased metabolic activities; these reports also showed that cancer cells' mitochondria further displayed increased rates of oxidative phosphorylation, higher membrane potential and enhanced calcium retention capacity [6,30,31]. The experiments reported here provide a comprehensive biophysical basis for the reported observations. In particular, we utilized inverted sub-mitochondrial particles (SMPs), prepared from mitochondria isolated from colon and prostate cells, which provided insight into membrane structures, dynamics, and enzyme functionality. In addition, spectroscopic and microscopic data reveal specific mitochondrial membrane interactions and targeting by betulinic acid and resveratrol, known anticancer agents, underscoring the likely prominent role of mitochondrial membranes in cancer cell properties and functions, and pointing to possible new therapeutic pathways centered on mitochondrial membranes.

2. Materials and methods

2.1. Materials

10-Doxyl nonadecane was purchased from Avanti Polar Lipids Inc. (Alabaster, AL USA). Cytochrome c (equine heart), cytochrome-c oxidase (bovine heart), DL-Dithiothreitol (DTT), 5-[(1E)-2-(4-Hydroxyphenyl)ethenyl]-1,3-benzenediol (resveratrol), 3β-Hydroxy-20(29)-lupaene-28-oic acid (betulinic acid) were obtained from Sigma Aldrich (Milwaukee, WI USA). MitoTracker Orange CM™ Ros purchased from Thermo Fisher Scientific (Waltham, MA, USA).

2.2. Cell cultures

Human colon cancer cells HCT 116 and human metastatic prostate cancer cells PC-3 were purchased from ATCC (Manassas, VA USA) at the available passage 60 and used up to 20 passages. Both cell lines were maintained in RPMI 1640 growth medium supplemented with 10% FBS. Human colon normal fibroblasts (CCD-18Co) were obtained at passage 2 from ATCC and maintained in EMEM medium with 10% FBS by passage 5. Primary human prostate epithelial cells (PrEC) were obtained at passage 2 from Lonza Inc. (Allendale, NJ USA). Cells were maintained in manufacturer recommended PrEGM medium with all required supplements except for gentamicin and were used by passage 5. The cells were grown at 37 °C in a humidified 5% CO_2 atmosphere at their log phase to maintain viable cell population and subsequently harvested at a confluence no larger than 80% to prevent induction of apoptosis.

2.3. Isolation of mitochondria from cultured cells

Mitochondria were isolated by differential centrifugation protocol described earlier [32]. For LC-MS analysis, the mitochondria pellet was additionally purified with Percoll gradient prepared in isolation buffer (75 mM mannitol, 225 mM sucrose, 10 mM MOPS, pH 7.2, 1 mM EGTA, 0.1% fatty acid free BSA). The crude mitochondria suspended in 15% Percoll was layered on 23% Percoll, which was then layered on 40% Percoll solution. After centrifugation for 35 min at 28,700 g, 4 °C in JA-20.1 Beckman rotor, the mitochondria band between the 23 and 40% Percoll was collected and rinsed in isolation buffer three times for 15 min at 17,000 g, 4 °C to remove Percoll residues. The final pellet was re-suspended in 100 μl of MiR05 respiration buffer (110 mM sucrose, 60 mM K-lactobionate, 20 mM HEPES, pH 7.2, 10 mM KH_2PO_4, 3 mM $MgCl_2x6H_2O$, 0.5 mM EGTA, 20 mM taurine, 0.1% fatty acid free BSA) [33] vortexed and stored in −80 °C prior to measurements. The mitochondrial protein content was determined by Bradford protein assay corrected for the BSA contained in the respiration buffer.

2.4. Lipid profiling by liquid chromatography-mass spectrometry (LC-MS)

For LC-MS studies, 100 μl of purified mitochondria lipid extracts were dried under vacuum at 40 mbar. 150 μl from acetonitrile\isopropanol\methanol solution (53:23:24) was added to each sample followed by 15 min bath sonication. The samples were then centrifuged for 5 min at 14,500 rpm and 150 μl of the upper phase were taken for analysis. Samples were processed using ultra-performance liquid chromatography (ACQUITY UPLC System; Waters (TC), Israel) coupled with Fourier transform mass spectrometry (UPLC/FT-MS) in negative ionization mode. UPLC separation was performed with a C18 reverse-phase column (100 × 2.1-mm inner diameter, 1.7-μm particle size; Waters) at 60 °C. For UPLC gradient the mobile phases consisted of two solvents: solvent A, acetonitrile, isopropanol, water, 1 M NH_4Ac (34:15:50:1%) and 0.1% acetic acid glacial; and solvent B, acetonitrile, isopropanol, 1 M NH_4Ac (69:30:1%) and 0.1% acetic acid glacial. Injection volume was 5 μl and the following gradient profile was applied: 1 min, 0% B (100%A); 4 min, linear gradient from 0% B to 44% B; 12 min, linear gradient from 44% B to 75% B; 15 min, linear gradient from 75% B to 100% B. The total run time was 24 min with a flow rate of the mobile phase of 0.4 ml min^{-1}. The mass spectra were acquired using an Exactive Orbitrap mass spectrometer (Thermo Fisher Scientific, Waltham, MA USA) and analyzed with LipidSearch™ software (Thermo Fisher Scientific) for identification of lipid types and acyl chains including alignment of chromatogram, chemical noise subtraction and intensity thresholding. All LC-MS measurements of lipid extracts were performed in 3 repetitions.

2.5. Preparation of mitochondrial lipid extracts

Multiple independent preparations of mitochondria were used for the experiments. Aliquots of each sample were dissolved separately in 5 ml chloroform:ethanol (1:1) solution. 1 ml 0.9% saline was added to induce lipid phase separation. Samples were then vortexed (3 repeats) at 180 rpm for 1 h at 30 °C, and the lower lipid-rich organic phase was collected. Solutions were further centrifuged at 3000 rpm for 15 min to remove impurities, followed by evaporation of organic solvent under vacuum at 40 mbar until a constant weight was attained. Samples of mitochondrial lipids were reconstituted in 1 ml chloroform and kept at -20 °C prior to analysis.

2.6. Preparation of submitochondrial particles (SMPs)

Inside-out submitochondrial particles (SMPs) were prepared according to an established protocol [34]. Briefly, suspensions of isolated mitochondria (20–30 mg protein/ml) were diluted with sonication buffer (250 mM sucrose, 10 mM Tris HCl, 1 mM EDTA, pH 7.2) to a

total of 2 ml volume. This suspension was probe-sonicated for 30 s on ice using 20% amplitude and six cycles of 5 s on/off sonication. Exclusion of Mg^{2+} ions by addition of EDTA enables to form inside-out oriented submitochondrial particles [35], in which the matrix side of the inner mitochondrial membrane inverts out to be exposed to experimental medium. The suspension of SMPs was then centrifuged at 8000 rpm to remove impurities including pieces of broken membranes. The protein content of SMPs (μg protein/ml) was determined by Bradford protein assay. The inversion of the inner mitochondrial membrane in SMP preparations was controlled by the cytochrome *c* oxidase (COX) test, using an additional control of non-inverted submitochondrial particles prepared by sonication in buffer containing Mg^{2+} ions (250 mM sucrose, 15 mM $MgSO_4$, 1 mM ATP, 10 mM MOPS, pH 7.2).

2.7. Zeta potential

ζ-Potential of SMPs was measured in 1 ml solutions in sonication buffer (250 mM sucrose, 10 mM Tris HCl, 1 mM EDTA, pH 7.2). The concentration of final suspension of SMPs was 90 μg protein/ml. Malvern DTS 1070 disposable capillary cuvettes were used for measurements in Zetasizer (Zetasizer Nano ZS, Malvern, Worcestershire, UK). Results are given as means of four replicates.

2.8. Cytochrome c oxidase enzyme activity

Cytochrome c oxidase (COX) activity was measured using the cytochrome *c* oxidase assay kit (Sigma Aldrich) spectroscopically by monitoring the decrease in absorbance at 550 nm of chemically reduced ferrocytochrome *c* solution in the presence of SMPs. Ferrocytochrome *c* substrate solution (final concentration 0.22 mM) was prepared by addition of 5 μM of 0.1 M DTT to 2.7 mg/ml cytochrome *c* enzyme dissolved in purified water. Samples of SMPs (50–200 μg protein/ml) or mixtures of SMPs (200 μg protein/ml) with increased concentrations of betulinic acid/resveratrol (5–100 μM) were supplemented with 950 μl of assay buffer (10 mM Tris HCl, 120 mM KCl, pH 7.0). The enzyme buffer (250 mM sucrose, 10 mM Tris HCl, pH 7.0) was then added in order to bring the total reaction volume to 1.1 ml. To compare the COX activity in normal and cancerous SMPs, all measurements were normalized for the positive control of pure cytochrome *c* oxidase enzyme (10 μg/ml). For evaluation of COX activity in the presence of betulinic acid/resveratrol, the results were normalized for a positive control of SMPs alone (200 μg protein/ml). To initiate the oxidation reaction between ferricytochrome *c* and cytochrome *c* oxidase, 50 μl of ferrocytochrome *c* substrate was added. Aliquots of 200 μl were measured in 5 repeats using 96-well plate. The kinetic changes of absorbance were measured for 20 min, with 20 s intervals at 25 °C on BioTek Synergy 4 microplate reader (Winooski, VT, USA). The activity of COX enzyme (units/ml) was calculated according to Eq. (1):

$$\text{COX activity}\left(\frac{\text{units}}{\text{mL}}\right) = \frac{\Delta A/\text{sec}\times\text{dil}\times V(t)}{V(s)\times 21.84}, \quad (1)$$

where ΔA/sec represents the reaction rate of a sample subtracted from the blank; dil refers to the dilution factor of ferrocytochrome *c* solution; V(t), total reaction volume; V(s) is the volume of ferrocytochrome *c* substrate added to initiate oxidation and 21.84 is the extinction coefficient between ferrocytochrome *c* and ferricytochrome *c* at 550 nm [36]. Unit definition: one unit oxidizes 1.0 μmol of ferrocytochrome *c* per sec at pH 7.0, 25 °C.

2.9. Electron paramagnetic resonance (EPR)

Samples for EPR study were prepared by mixing the 10-doxyl nonadecane (10-doxyl) radical spin probe with SMPs in a molar ratio of about 400:1 (phospholipid: spin probe). 200 μg protein/ml of different cancer and normal SMPs or mixture of SMPs with betulinic acid or resveratrol (0–100 μM) were assessed. Control measurements were carried out in the presence of DMSO in the same volumes as used with the tested solutions. Samples were placed in 20 mm length, 1 mm internal-diameter quartz capillary and continuous wave X-band (9.4 GHz) EPR measurements were carried out using Bruker EMX220 spectrometer (Bruker, Germany) operated at room temperature. Spectra were recorded at 20 mW microwave power, 100 kHz modulation amplitude of 0.1 mT and 2×10^6 receiver gain. Sweep width was 12 mT, number of data points was 1024 and number of coherent acquisition scans was 100. Data processing was carried out using Bruker's WIN-EPR and OriginLab (OriginLab Corporation, USA) softwares. Eq. (2) was used to determine the rotational correlation time (τ_c):

$$\tau_c = 6.5\times 10^{-10}\cdot \triangle H_{pp(0)}\left(\sqrt{A_{(0)}/A_{(-1)}} - 1\right)(sec), \quad (2)$$

where τ_c is the rotational correlation time (sec), 6.5×10^{-10} is the constant derived using the magnetic parameters of a small water-soluble nitroxide, t-butyl nitroxide spin label; $\triangle H_{pp(0)}$ is the peak to peak width of the center line; $A_{(0)}$ and $A_{(-1)}$ are the peak-to-peak heights of the center- and high-field lines, respectively [37]. Experimental errors for the correlation time values were determined as standard deviations (± SD) obtained from nine independent EPR measurements done on the same sample.

2.10. Confocal imaging

Cells were seeded on 0.8 cm^2 micro-slides (Nunc™ Lab-Tek™, ThermoFisher Scientific, USA) at a density of 2×10^4 cells per well and maintained overnight. Prior to imaging, cells were incubated with 1 mM resveratrol in the growth medium for 30 min at 37 °C and then rinsed with PBS (containing Ca^{2+} and Mg^{2+}). Subsequently, cells were stained with 20 nM MitoTracker Orange CM™Ros for 30 min at 37 °C. Images were acquired on Zeiss LSM880 confocal microscope (Germany), using CLSM plan-Aprochromat, ×20/0.8 M27 objective. Excitation/emission wavelengths of resveratrol and MitoTracker Orange were 405/448 nm and 561/566 nm, respectively.

3. Results

3.1. Cancer-induced changes in mitochondrial membrane properties

The objective of this study is to elucidate the changes in mitochondrial membrane properties in colon cancer/prostate cancer cells and evaluate the functional implications of those membrane transformations. Fig. 1 presents compositional analyses of mitochondrial membranes extracted from human primary prostate epithelial cells (PrEC), human prostate cancer (PC-3) cell line, human colon normal (CCD-Co18) and cancer (HCT 116) cell lines. The mitochondrial membranes were assessed by liquid chromatography-mass spectrometry (LC-MS) to analyze both lipid compositions and acyl chain profiles. Fig. 1A depicts the relative abundance of zwitterionic lipids [including phosphatidylcholine (PC), phosphatidylethanolamine (PE) and sphingomyelin (SM)], negative lipids excluding cardiolipin (CL) (without CL) [phosphatidylglycerol (PG), phosphatidylinositol (PI), phosphatidylserine (PS) and phosphatidic acid (PA)] and solely cardiolipin (CL), a prominent lipid constituent of mitochondrial membranes [38] (percentages of individual lipids are depicted in Suppl. Fig. 1S).

Differences between cancer and normal membranes were apparent in mitochondria isolated from either prostate or colon cells. Specifically, a small increase of around 2% was recorded in CL content of normal colon cells' mitochondria, while a dramatic increase of approximately 14% was recorded in cancer cells. In prostate cells' mitochondria, the comparative values were 1% (normal cells) and 9% in cancer cell. CL is known for promoting incorporation of integral proteins inside the inner mitochondrial membrane [39], including respiratory protein complexes [38], adenine nucleotide transporter [40],

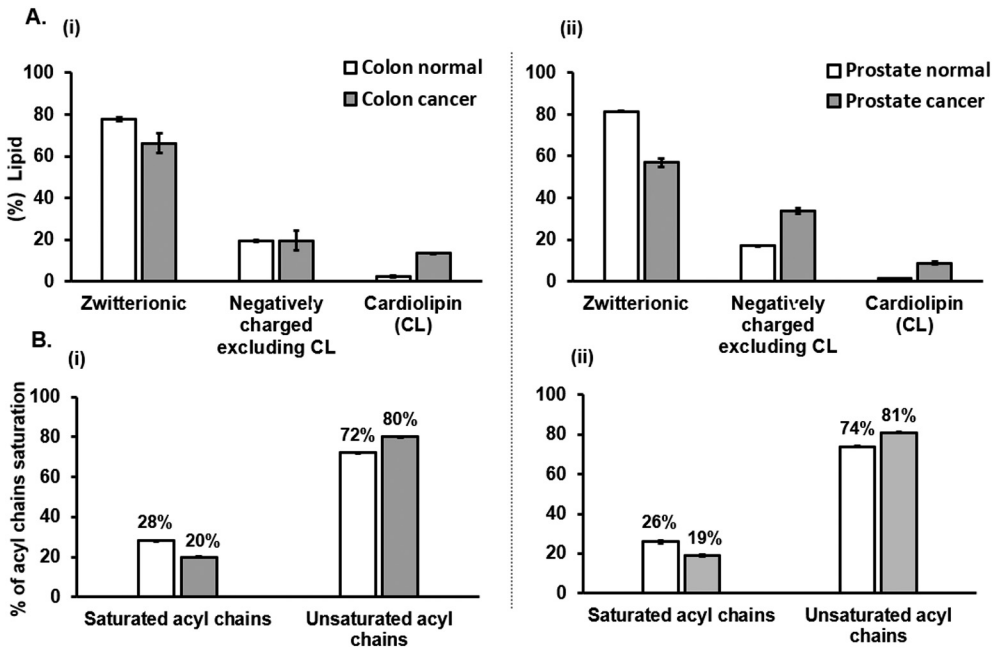

Fig. 1. Analysis of lipid and acyl chain compositions in human colon and prostate mitochondrial extracts. A. Mitochondrial lipid compositions presented in the following groups: zwitterionic lipids, negatively charged excluding cardiolipin (CL), and CL only. (i) Colon cancer (HCT 116) vs normal (CCD-Co18) mitochondria; (ii) prostate cancer cells (PC-3) vs normal (PrEC) cells' mitochondria. Data are presented as mean ± SD (n = 3). B. Distribution of unsaturated and saturated acyl chains in colon (i) and prostate (ii) lipid extracts. The standard deviations in all the data presented in B are less than 1%.

creatine and nucleoside diphosphate kinases [41], linking this lipid constituent with increased mitochondrial energy metabolism in cancer cells.

In parallel with the pronounced increase in cancer-associated CL concentration, a decrease in the percentage of zwitterionic lipids was detected in both types of mitochondria (Fig. 1A). Specifically, in colon mitochondria lipid extracts, the concentration of zwitterionic lipids was 66% in cancer cells vs 77% in normal cell samples, while in the case of prostate cells' mitochondria the corresponding percentage values were 57% vs 82%. The changes in zwitterionic and negative lipids in both types of cancer correlated with the higher abundance of CL, which exhibits the more spacious hexagonal phase in lipid bilayers [42]. The level of CL was higher in colon cancer cells than in prostate cancer samples resulting in a lower decrease in zwitterionic lipids than those in prostate cancer cells, with the negative lipids (other than CL) remaining seemingly unaltered. In contrast, in prostate cancer mitochondria the concentration of negative lipids (other than CL) significantly increased (Fig. 1A,ii). This increase correlated with a lower concentration of zwitterionic lipids than observed in colon cancer. It is important to note that colon cancer lipidomics exhibited greater variability and linked to subsites and tumor locations [43].

Membrane architecture and dynamic properties intimately depend on the type, and particularly saturation of lipid acyl chains. Fig. 1B summarizes the degrees of acyl chain saturation in the mitochondrial membranes of the cells studied. Notably, mitochondria isolated from cancer cells in both tissues contained lower concentrations of saturated acyl chains compared to mitochondria from normal cells (20% vs 28% in colon samples, Fig. 1B,i; 19% vs 26% in prostate samples, Fig. 1B,ii; the distributions of specific acyl chains are shown in Suppl. Fig. 2S). The compositional changes of mitochondrial membranes in colon cancer and prostate cancer apparent in Fig. 1, particularly the dramatic increase in the abundance of CL and lower acyl chain saturation, have not been previously reported. Indeed, the enhanced fluidity of cancer mitochondrial membranes may promote accommodation of elevated concentrations of membrane-associated proteins responsible for respiration and energy production in prostate and colon cancers.

CL is primarily localized in the inner mitochondrial membrane, in which it is tightly associated with respiration proteins [44]. To obtain additional insight into the properties of the inner mitochondrial membrane leaflets we prepared inverted submitochondrial particles (SMPs) and carried out structural and functional analysis of these particles [45] (Figs. 2–3). SMPs, prepared via probe-sonication of isolated mitochondrial suspensions in the presence of EDTA, exhibit "inside-out" orientation exposing the inner mitochondrial membrane and embedded proteins [34]. Representative images of SMPs prepared from prostate mitochondria carried out by transmission electron microscopy (TEM) (Suppl. Fig. 3S). As such, SMPs have been employed in varied mitochondria analyses as they present integrated systems containing both protein and lipid constituents of the inner mitochondrial membrane.

The zeta potentials recorded for the SMPs in Fig. 2A attest to significant modulation of surface charges in cancer mitochondria. Specifically, in case of SMPs prepared from colon cells, the zeta potential decreased from −19 mV in normal mitochondria to −25 mV in cancer mitochondria, while a similarly significant drop was recorded for prostate cancer SMPs (from −16 mV to −22 mV). The higher negative charges displayed upon the surface of SMPs prepared from both colon and prostate cancer cells are consistent with the greater abundance of CL and anionic lipids in cancer mitochondrial membranes inferred from the LC-MS analysis (e.g. Fig. 1).

EPR analysis represented in Fig. 2B furnish important information on cancer-associated changes in mitochondrial membrane dynamics. In the experiments, we employed the spin probe 10-doxyl nonadecane (10-doxyl) which partitions closer to the membrane bilayer core, thereby illuminating their dynamic properties [46]. The bar diagram in Fig. 2B,i depicts the rotation correlation times (τ_c) of 10-doxyl, calculated from the EPR spectra presented at Fig. 2B,ii [37], (the parameters extracted from the EPR spectra upon which the τ_c values were calculated are provided in Suppl. Table 1S) following 20 min incubation with the SMPs prepared from either colon and prostate samples. Notably, when SMPs were incubated with 10-doxyl, higher τ_c values were recorded in colon and in prostate cancer mitochondria compared to the SMPs prepared from normal cells. This result, indicative of more rigid SMP membranes, likely corresponds to the higher abundance of mitochondrial membrane proteins accommodated in the inner mitochondrial membranes in cancer cells [47–50]. Fluorescence anisotropy results employing 1,6-diphenylhexatriene (DPH) which similarly penetrates into the bilayers corroborate the greater rigidity in cancer SMPs (Suppl. Fig. 5S).

We further explored the functional aspects of mitochondrial membranes in prostate and colon cells (Fig. 3). Fig. 3A depicts the activity of cytochrome *c* oxidase (COX) in inverted SMPs prepared from normal and cancer mitochondria, respectively. COX has a central role in

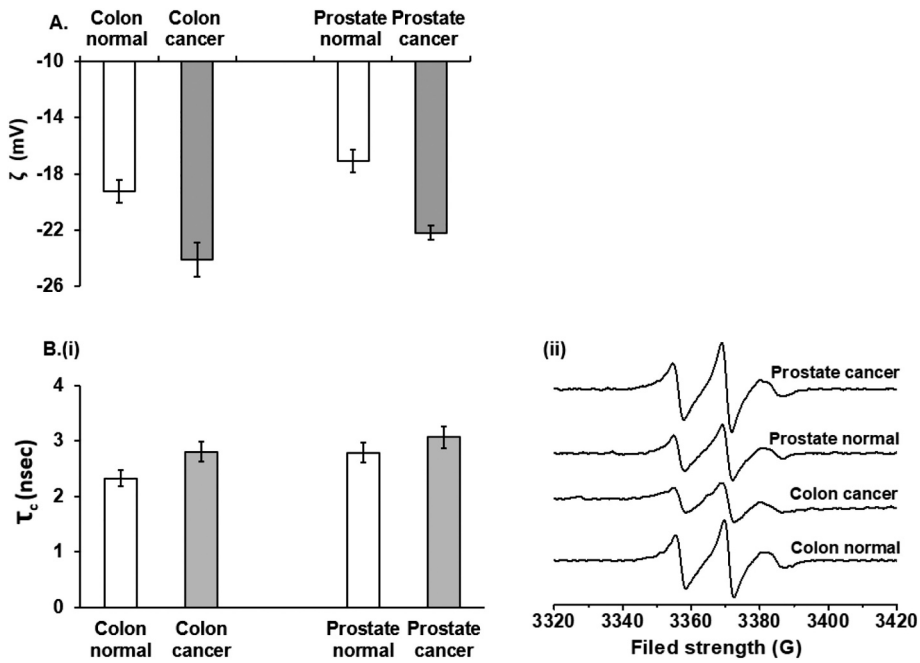

Fig. 2. Structural and dynamic properties of inverted submitochondrial particles (SMPs). A. Zeta potential analysis. Data are presented as mean ± SD (n = 3). B (i). Rotation correlation times (τ_c) extracted from the EPR spectra (shown in ii) recorded for 10-doxyl nonadecane incubated with colon and prostate SMPs.

mitochondria-mediated respiration as this protein comprises the terminal complex in the respiration pathway and the structural and dynamical properties of the mitochondrial membrane intimately affect the efficiency of electron transport mediated by this enzyme [51]. Indeed, Fig. 3 demonstrates that in all inverted SMP concentrations examined, COX activity was significantly higher in cancer SMPs in both colon (Fig. 3A) and prostate cells (Fig. 3B). This result is consistent with the elevated expression of mitochondrial proteins, including COX, required to maintain the high energy demands of cancer cells [52,53]. Interestingly, COX activity in colon mitochondria (both normal and cancer cells) (Fig. 3A) was significantly higher than in prostate mitochondria (Fig. 3B). This observation may correlate with the higher content of CL in colon cancer mitochondria (e.g. Fig. 1), accommodating a greater concentration of the enzyme in the inner mitochondrial membrane in colon cancer cells compared to prostate cells. Control experiments confirm lack of COX activity in non-inverted SMPs (Suppl. Fig. 4S).

3.2. Membrane interactions of mitochondria-targeting compounds

While Figs. 1–3 illuminate cancer-induced changes in mitochondrial membrane properties, we further investigated the effect of molecules exhibiting therapeutic potential against cancer on mitochondrial membrane organization and functionality (Figs. 4–5). Fig. 4 examines the effects of betulinic acid, a plant-derived pentacyclic triterpenoid known to induce apoptosis in cancer cells via altering mitochondrial permeability [54], upon membrane dynamics and functionalities. In the experiments outlined in Fig. 4A and B 10-doxyl was incubated for 20 min with SMPs prepared from normal and cancer cells and the changes in the rotation correlation time with betulinic/DMSO ($\tau_{c\ (i)}/\tau_{c\ (0)}$) were quantified. DMSO served as a control according to which the values were normalized. The bar diagrams in Fig. 4A,i and B,i demonstrates that betulinic acid gave rise to significant, dose-dependent increase in 10-doxyl rotation correlation times ratios upon incubation with SMPs obtained from cancer cells (both colon and prostate cancers, Fig. 4A,i, and B(i) respectively, grey bars). This result likely accounts for the affinity of betulinic acid to CL [55], resulting in insertion into the membrane and concomitant higher rigidity. Notably, no effect upon 10-doxyl correlation time ratio was apparent when betulinic acid was added to SMPs prepared from normal colon cells (Fig. 4A,i, white bars), and no significant change in correlation time ratio was also recorded in the case of normal prostate cells (Fig. 4B,i, white bars). The EPR spectra upon which the rotation correlation times were calculated are presented as well; pertinent parameters extracted from the spectra are provided in Suppl. Tables 2S and 3S.

Fig. 4C depicts the effect of betulinic acid upon COX activity in SMPs prepared from colon and prostate cells' mitochondria, respectively. The graph in Fig. 4C shows a dramatic dose-dependent decrease in COX activity induced upon incubation of cancer cell-derived SMPs with betulinic acid (Fig. 4C, red traces). The pronounced inhibition of COX activity was apparent both in colon cancer SMPs (solid red line, Fig. 4C) and prostate cancer SMPs (broken red line, Fig. 4C). The reduced enzymatic activity of COX possibly corresponds to CL-induced

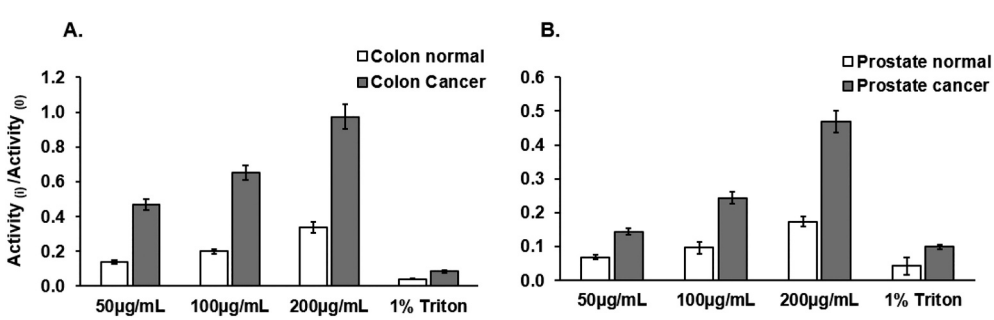

Fig. 3. Enzymatic activity of cytochrome *c* oxidase (COX) in colon and prostate SMPs. A. Activities of COX recorded in inverted SMPs prepared from normal and cancer colon cell mitochondria. B. COX activity in normal and cancer prostate mitochondria. The Y axis values correspond to enzyme activity ratios measured in different SMPs. 1% Triton X was added to SMPs (200 μg/ml) and used as a negative control. Data are presented as mean ± SD (n = 3).

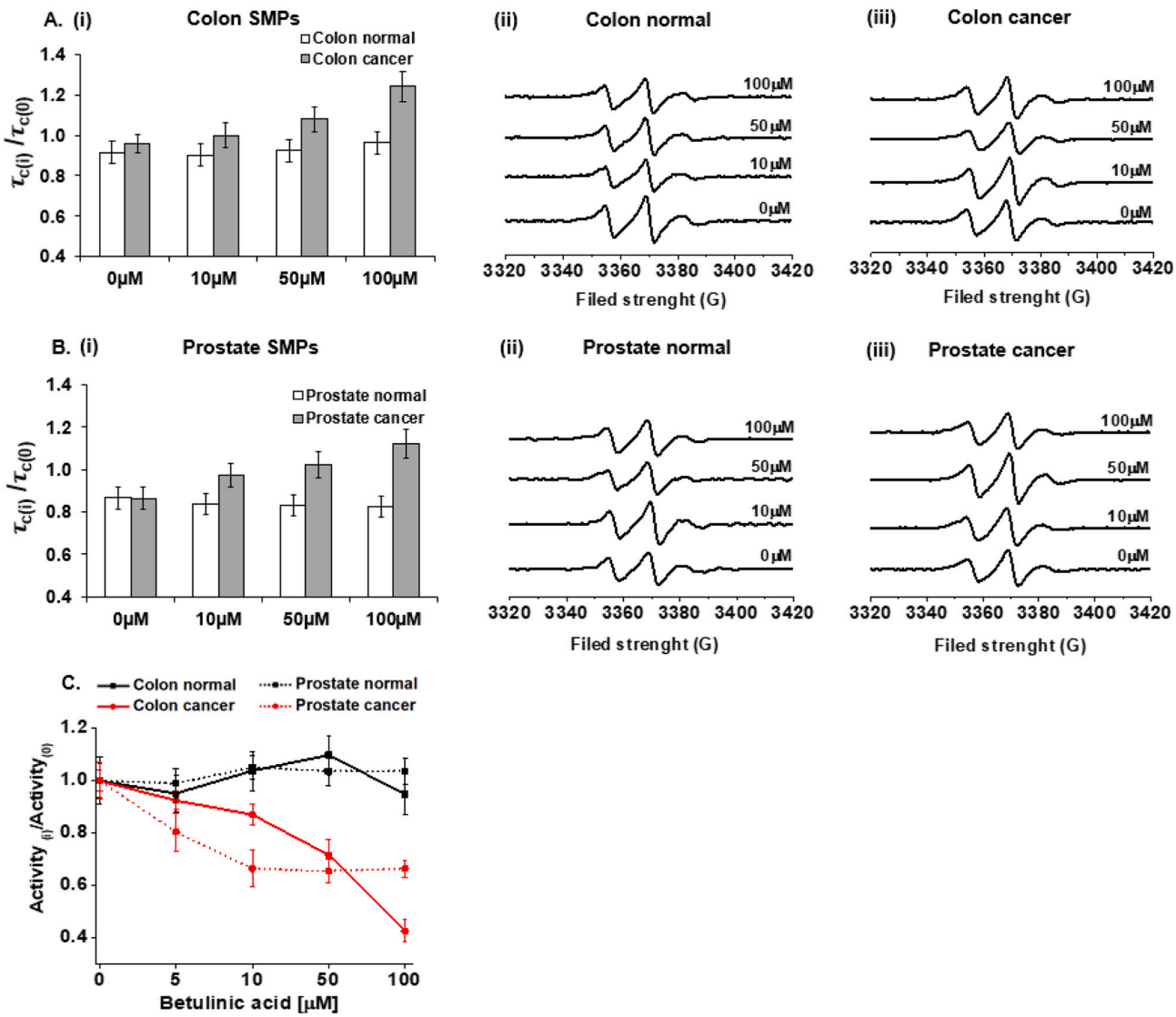

Fig. 4. Interactions of betulinic acid with inverted submitochondrial particles (SMPs). A (i) Rotation correlation time ratios calculated from the EPR spectra (shown on the right) recorded for 10-doxyl incubated with colon SMPs following addition of different concentrations of betulinic acid; B(i) Rotation correlation time ratios of prostate SMPs (The original EPR spectra are shown on the right) C. COX activity recorded in colon and prostate SMPs following addition of different concentrations of betulinic acid. Data are presented as mean ± SD (n = 3). The Y axis corresponds to the COX enzyme activity ratio.

insertion of betulinic acid into the mitochondrial membrane (e.g. the EPR data in Fig. 4A,i and B,i), thereby disrupting the bilayer ordering and activity of membrane-associated integral proteins, in particular CL-associated COX [56]. Cancer mitochondrial membranes are more rigid than the normal membrane. Addition of high dose betulinic acid (100 μM) further increased bilayer rigidity (Fig. 4A,i and B,i). Indeed, the most pronounced COX inhibition effect was observed at the highest concentration of betulinic acid (Fig. 4C). However, direct interaction of betulinic acid with COX may also occur since the enzymatic activity started declining in the presence of lower concentration of betulinic acid, even before bilayer modifications occurred. Notably, the graph in Fig. 4C demonstrates that betulinic acid had no effect upon COX activity in SMPs prepared from normal colon or prostate mitochondria (Fig. 4C, black lines); this result is similarly consistent with the EPR results in Fig. 4A,B,i which indicate minimal embedding of betulinic acid within normal cells' mitochondrial membranes which contain significantly lower CL concentration than cancer cells' mitochondria.

To complement the experimental data in Fig. 4 depicting the effects of betulinic acid upon mitochondrial membranes, we also examined mitochondrial membrane targeting by resveratrol fluorescence microscopy in living cells (Fig. 5A) and in mitochondrial membranes by measuring the COX activity (Fig. 5B). Resveratrol is a natural polyphenol derived from red grapes and blueberries, shown to accumulate in mitochondria of malignant cells, inhibits mitochondria respiratory activity, contributes to ROS production, and induces apoptosis [57,58]. In the confocal microscopy experiments depicted in Fig. 5A, colon and prostate cancer cells stained with the mitochondria-specific fluorescent dye MitoTracker Orange were co-incubated with resveratrol. The cells were then imaged in dual colors, depicting resveratrol (green) and MitoTracker Orange (red) fluorescence emission. As shown in Fig. 5A, resveratrol and MitoTracker Orange are colocalized, confirming uptake of resveratrol by mitochondria in cancer cells.

Fig. 5B depicts the influence of resveratrol upon COX activity in SMPs prepared from normal and cancerous colon/prostate cells. The graph in Fig. 5B demonstrates dose-response resveratrol-correlated decrease in COX activity induced upon incubation of cancer cell-extracted SMPs with the compound (Fig. 5B, red lines). Essentially, Fig. 5B highlights the same phenomenon observed in Fig. 4B, i.e. pronounced inhibition of COX activity apparent both in colon cancer SMPs (solid red lines, Fig. 5B) and prostate cancer SMPs (broken red lines,

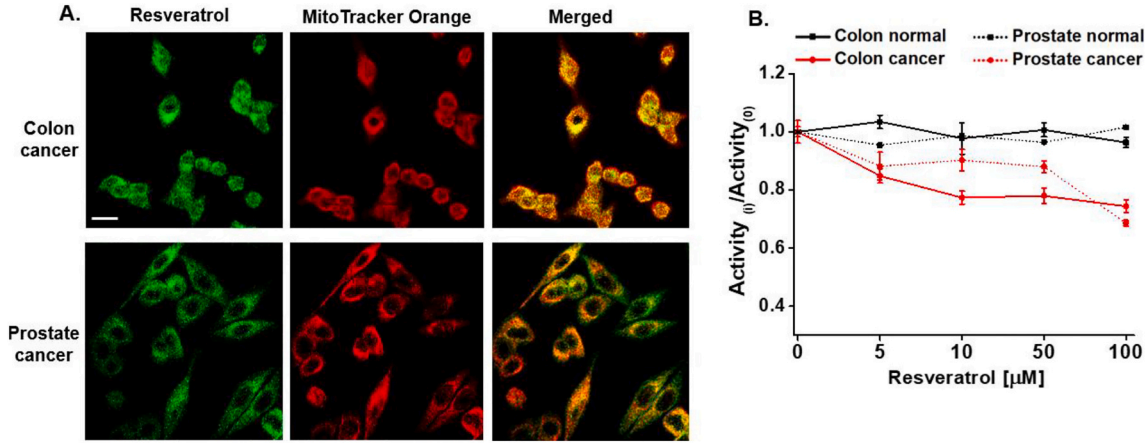

Fig. 5. Targeting of cancer mitochondria by resveratrol. A. Confocal fluorescence microscopy images of colon cancer cells (HCT 116) and prostate cancer cells (PC-3) treated with resveratrol (final concentration 1 mM). Following incubation with resveratrol the cells were stained with MitoTracker Orange and images were recorded (Ex/Em of resveratrol and MitoTracker Orange were 405/448 nm and 561/566 nm, respectively). Scale bar corresponds to 20 μm. B. COX activity measured in colon and prostate SMPs following addition of different resveratrol concentrations. Data are presented as mean ± SD (n = 3). The Y axis corresponds to the COX enzyme activity ratio.

Fig. 5B). Lesser mitochondria localization of resveratrol was apparent in Hek293 cells, selected as a model for normal cells (Suppl. Fig. 6S), consistent with the specific association of resveratrol with cancerous mitochondrial membranes.

4. Discussion

Cancer research and therapeutics development have, to an extent, overlooked the mitochondria, despite of their central role in cell metabolism and apoptosis. While some mitochondria-associated proteins have attracted interest in cancer studies due to their roles in respiration and cell death processes, the interplay between mitochondrial membranes and cancer has not been thoroughly investigated. In general, lipids consist around 30% of cell membrane constituents, and in mitochondria the phospholipid/protein ratio is even lower [59,60]. However, lipid composition, distribution, and dynamic properties are critical determinants for mitochondrial functionality. This study examines cancer-associated structural and functional changes in mitochondrial membranes of colon and prostate cells. Our aim is to illuminate the relationship between malignancy and important parameters pertaining to mitochondrial membranes, including lipid profile, membrane surface charge and fluidity, functionality of membrane-embedded proteins, and interactions of the membranes with known anticancer compounds.

Lipid compositions of the mitochondrial membranes in both colon and prostate tissues, analyzed by LC-MS, were significantly different in normal and cancer cells in the two cancer types investigated. In particular, dramatic increase in CL concentrations (which is between 8 and 12% of total mitochondrial membranes lipids [59,61]) and decrease in zwitterionic phospholipids were recorded in cancerous cell mitochondria, both in case of colon cancer and prostate cancer. These results are important since almost all cancer cell lipid profiles reported in the literature were carried out for whole cell or tissue extracts, rather than the mitochondrial membranes only [18,62]. Previous studies indicated CL alterations in different types of brain tumor [26] and decreased CL associated with impaired mitochondria functions in hepatoma cells [63]. The increase in CL concentration in cancer cells is notable as this lipid significantly affects membrane curvature, structure, fluidity, cristae stability and incorporation of membrane proteins [64]. Furthermore, CL has been shown to complex with cytochrome *c*, a well-known apoptotic trigger, thereby inhibiting release of cell death proteins [65].

The significantly higher concentration of CL in mitochondrial membranes of cancer cells, (Fig. 1A), together with the decrease in lipid acyl chain saturation both in prostate cancer and colon cancer mitochondria (Fig. 1B), promote incorporating higher concentrations of mitochondrial membrane integral proteins such as COX, which play critical roles in proliferation of cancer cells [66]. The significance of CL for COX electron transport activity was demonstrated with stoichiometry of two-to-four CL molecules per one dimeric enzyme [67]. Thus, greater abundance of CL in cancer mitochondria likely serves as extensive scaffolding for embedding the enzyme and forming ubiquitous multiprotein electron transport complexes. Indeed, the EPR analysis in Fig. 2 indicates more pronounced rigidity of cancerous mitochondrial membranes, and the enzyme functionality experiments in Fig. 3 reveal higher COX activity in SMPs derived from colon cancer cells and prostate cancer cells. Previous studies also reported elevated COX expression and enzymatic activities in colon and prostate cancers [6,30].

Utilization of SMPs in the mitochondrial membrane study carried out here is notable. While the outer and inner mitochondrial membranes differ compositionally and functionally, both are important for mitochondria functionality. The inner mitochondrial membrane, in particular, is the primary site of energetic processes [68]. Accordingly, inverted SMPs, reconstructed from intact mitochondria and thus containing both lipid and protein components of the membrane, constitute an invaluable bioanalytical tool allowing examination of the inner lipid leaflet [35].

As our data attest to significant cancer-induced modification of mitochondrial membranes, targeting of these membranes may have therapeutic benefit. Indeed, experiments carried out with betulinic acid and resveratrol, compounds investigated as potential anti-cancer therapeutics, underscore their specific association and structural/functional effects upon the mitochondrial membranes of cancer cells. In particular, betulinic acid suppressed COX activity in both colon and prostate cancer SMPs (Fig. 4), while minimal effect was apparent in case of normal cells from these tissues. Previous studies reported affinity of betulinic acid to lipid monolayers mimicking mitochondrial membrane compositions, pointing to possible interactions of the compound with the anionic headgroups of CL [55]. The EPR data in Fig. 4 similarly indicate high affinity of betulinic acid to SMPs extracted from cancer mitochondria. Resveratrol was also found to be attracted to mitochondrial membranes in prostate and colon cancer cells and to inhibit the activity of one of mitochondrial key enzymes COX (Fig. 5). Our data are consistent with the reported inhibition of cancer cells' growth affected by resveratrol, believed to occur via mitochondria-mediated mechanisms [69].

5. Conclusions

This study illuminates distinct structural and functional transformations of mitochondrial membranes occurring in prostate and colon cancer cells. Mass spectrometry reveals significant modification of lipid compositions and acyl chain saturation, particularly pronounced increase in cardiolipin concentration and higher lipid unsaturation. These compositional modulations, recorded both in case of prostate cancer and colon cancer mitochondria, translate to greater uptake of mitochondrial integral membrane proteins. This process results in enhanced rigidity and higher enzyme activity in cancer cells' mitochondria, measured in this work in case of cytochrome *c* oxidase, a prominent mitochondrial protein involved in cell energy metabolism.

Importantly, SMPs prepared from mitochondria isolated from colon and prostate cells, the main experimental platform employed here, provided important insight into properties of the actual mitochondrial inner membrane, and changes to membrane properties induced by the onset of cancer. In particular, the SMP experiments in cancer samples indicated greater membrane rigidity, more pronounced anionic lipid headgroups, and higher activity of COX. These changes likely contributed to the specific mitochondrial membrane interactions and mitochondrial targeting by betulinic acid and resveratrol, known anticancer agents. Overall, this work highlights the significant transformations of mitochondrial membranes incurred in colon and prostate cancers, pointing to possible new therapeutic pathways centered on mitochondrial membranes.

CRediT authorship contribution statement

S.B.Z., R.J., Z.O. and S.K. conceived the idea and designed the experiments; S.B.Z, S.K, A.I.S., E.A.S and E.D. performed the research; S.B.Z., R.J., Z.O, S.K., J.L.P., D.E.S. analyzed the data and wrote the manuscript. All authors edited the manuscript and approved the final version.

Declaration of competing interest

The authors declare that they have no known competing financial interests or personal relationships that could have appeared to influence the work reported in this paper.

Acknowledgments

Financial support from the Louis and Bessie Stein Family Fellowship to Drs. Jelinek and Poggio is acknowledged.

Appendix A. Supplementary data

Supplementary data to this article can be found online at https://doi.org/10.1016/j.bbamem.2020.183471.

References

[1] R.L. Siegel, K.D. Miller, A. Jemal, Cancer statistics, 2020, CA Cancer J. Clin. 70 (2020) 7–30.
[2] R.L. Siegel, K.D. Miller, A. Goding Sauer, S.A. Fedewa, L.F. Butterly, J.C. Anderson, A. Cercek, R.A. Smith, A. Jemal, Colorectal cancer statistics, 2020, CA Cancer J. Clin. 70 (2020) 145–164.
[3] H. Maeda, M. Khatami, Analyses of repeated failures in cancer therapy for solid tumors: poor tumor-selective drug delivery, low therapeutic efficacy and unsustainable costs, Clin Transl Med 7 (2018) 11.
[4] J.S. Carew, P. Huang, Mitochondrial defects in cancer, Mol. Cancer 1 (2002) 9.
[5] E.D. Lagadinou, A. Sach, K. Callahan, R.M. Rossi, S.J. Neering, M. Minhajuddin, J.M. Ashton, S. Pei, V. Grose, K.M. O'Dwyer, J.L. Liesveld, P.S. Brookes, M.W. Becker, C.T. Jordan, BCL-2 inhibition targets oxidative phosphorylation and selectively eradicates quiescent human leukemia stem cells, Cell Stem Cell 12 (2013) 329–341.
[6] A. Panov, Z. Orynbayeva, Bioenergetic and antiapoptotic properties of mitochondria from cultured human prostate cancer cell lines PC-3, DU145 and LNCaP, PLoS One 8 (2013) e72078.
[7] B.B. Zhang, D.G. Wang, F.F. Guo, C. Xuan, Mitochondrial membrane potential and reactive oxygen species in cancer stem cells, Familial Cancer 14 (2015) 19–23.
[8] L.B. Sullivan, N.S. Chandel, Mitochondrial reactive oxygen species and cancer, Cancer Metab 2 (2014) 17.
[9] C. Corbet, A. Pinto, R. Martherus, J.P. Santiago de Jesus, F. Polet, O. Feron, Acidosis drives the reprogramming of fatty acid metabolism in cancer cells through changes in mitochondrial and histone acetylation, Cell Metab. 24 (2016) 311–323.
[10] D.R. Wise, R.J. DeBerardinis, A. Mancuso, N. Sayed, X.Y. Zhang, H.K. Pfeiffer, I. Nissim, E. Daikhin, M. Yudkoff, S.B. McMahon, C.B. Thompson, Myc regulates a transcriptional program that stimulates mitochondrial glutaminolysis and leads to glutamine addiction, Proc. Natl. Acad. Sci. U. S. A. 105 (2008) 18782–18787.
[11] L. Bubendorf, G. Sauter, H. Moch, P. Jordan, A. Blochlinger, T.C. Gasser, M.J. Mihatsch, Prognostic significance of Bcl-2 in clinically localized prostate cancer, Am. J. Pathol. 148 (1996) 1557–1565.
[12] L. Biasutto, L.F. Dong, M. Zoratti, J. Neuzil, Mitochondrially targeted anti-cancer agents, Mitochondrion 10 (2010) 670–681.
[13] S. Beloribi-Djefaflia, S. Vasseur, F. Guillaumond, Lipid metabolic reprogramming in cancer cells, Oncogenesis 5 (2016) e189.
[14] X. Luo, C. Cheng, Z. Tan, N. Li, M. Tang, L. Yang, Y. Cao, Emerging roles of lipid metabolism in cancer metastasis, Mol. Cancer 16 (2017) 76.
[15] A. Pakiet, J. Kobiela, P. Stepnowski, T. Sledzinski, A. Mika, Changes in lipids composition and metabolism in colorectal cancer: a review, Lipids Health Dis. 18 (2019) 29.
[16] F. Podo, Tumour phospholipid metabolism, NMR Biomed. 12 (1999) 413–439.
[17] G.V. Sherbet, Membrane fluidity and cancer metastasis, Exp Cell Biol 57 (1989) 198–205.
[18] I. Dobrzynska, B. Szachowicz-Petelska, S. Sulkowski, Z. Figaszewski, Changes in electric charge and phospholipids composition in human colorectal cancer cells, Mol. Cell. Biochem. 276 (2005) 113–119.
[19] S. Ran, P.E. Thorpe, Phosphatidylserine is a marker of tumor vasculature and a potential target for cancer imaging and therapy, Int. J. Radiat. Oncol. Biol. Phys. 54 (2002) 1479–1484.
[20] P. Maycotte, A. Marin-Hernandez, M. Goyri-Aguirre, M. Anaya-Ruiz, J. Reyes-Leyva, P. Cortes-Hernandez, Mitochondrial dynamics and cancer, Tumour Biol. 39 (2017) (1010428317698391).
[21] F. Feo, R.A. Canuto, G. Bertone, R. Garcea, P. Pani, Cholesterol and phospholipid composition of mitochondria and microsomes isolated from Morris hepatoma 5123 and rat liver, FEBS Lett. 33 (1973) 229–232.
[22] R. Morton, C. Cunningham, R. Jester, M. Waite, N. Miller, H.P. Morris, Alteration of mitochondrial function and lipid composition in Morris 7777 hepatoma, Cancer Res. 36 (1976) 3246–3254.
[23] C.M. Julienne, M. Tardieu, S. Chevalier, M. Pinault, P. Bougnoux, F. Labarthe, C. Couet, S. Servais, J.F. Dumas, Cardiolipin content is involved in liver mitochondrial energy wasting associated with cancer-induced cachexia without the involvement of adenine nucleotide translocase, Biochim. Biophys. Acta 1842 (2014) 726–733.
[24] J. Montero, A. Morales, L. Llacuna, J.M. Lluis, O. Terrones, G. Basanez, B. Antonsson, J. Prieto, C. Garcia-Ruiz, A. Colell, J.C. Fernandez-Checa, Mitochondrial cholesterol contributes to chemotherapy resistance in hepatocellular carcinoma, Cancer Res. 68 (2008) 5246–5256.
[25] R. Garcea, R.A. Canuto, B. Gautero, M. Biocca, F. Feo, Phospholipid composition of inner and outer mitochondrial membranes isolated from Yoshida hepatoma AH-130, Cancer Lett. 11 (1980) 133–139.
[26] M.A. Kiebish, X. Han, H. Cheng, J.H. Chuang, T.N. Seyfried, Cardiolipin and electron transport chain abnormalities in mouse brain tumor mitochondria: lipidomic evidence supporting the Warburg theory of cancer, J. Lipid Res. 49 (2008) 2545–2556.
[27] C.E. Park, C.E. Wenner, Mitochondrial lipids of Ehrlich Lettre ascites tumor cells, Oncology 24 (1970) 241–260.
[28] S. Lucken-Ardjomande, S. Montessuit, J.C. Martinou, Bax activation and stress-induced apoptosis delayed by the accumulation of cholesterol in mitochondrial membranes, Cell Death Differ. 15 (2008) 484–493.
[29] M.A. Kiebish, X. Han, H. Cheng, A. Lunceford, C.F. Clarke, H. Moon, J.H. Chuang, T.N. Seyfried, Lipidomic analysis and electron transport chain activities in C57BL/6J mouse brain mitochondria, J. Neurochem. 106 (2008) 299–312.
[30] O. Altinok, J.L. Poggio, D.E. Stein, W.B. Bowne, A.C. Shieh, N.W. Snyder, Z. Orynbayeva, Malate-aspartate shuttle promotes L-lactate oxidation in mitochondria, J. Cell. Physiol. 235 (2020) 2569–2581.
[31] A. Kaldma, A. Klepinin, V. Chekulayev, K. Mado, I. Shevchuk, N. Timohhina, K. Tepp, M. Kandashvili, M. Varikmaa, A. Koit, M. Planken, K. Heck, L. Truu, A. Planken, V. Valvere, E. Rebane, T. Kaambre, An in situ study of bioenergetic properties of human colorectal cancer: the regulation of mitochondrial respiration and distribution of flux control among the components of ATP synthasome, Int. J. Biochem. Cell Biol. 55 (2014) 171–186.
[32] A.V. Panov, S. Lund, J.T. Greenamyre, Ca2+-induced permeability transition in human lymphoblastoid cell mitochondria from normal and Huntington's disease individuals, Mol. Cell. Biochem. 269 (2005) 143–152.
[33] A.V. Kuznetsov, G. Brandacher, W. Steurer, R. Margreiter, E. Gnaiger, Isolated rat heart mitochondria and whole rat heart as models for mitochondrial cold ischemia-reperfusion injury, Transplant. Proc. 32 (2000) 45.
[34] C. Lee, Tightly coupled beef heart submitochondrial particles, Methods Enzymol. 55 (1979) 105–112.
[35] C. Lee, L. Ernster, Energy-coupling in nonphosphorylating submitochondrial particles, Methods Enzymol. 10 (1967) 543–548.
[36] E.A. Berry, B.L. Trumpower, Simultaneous determination of hemes a, b, and c from

pyridine hemochrome spectra, Anal. Biochem. 161 (1987) 1–15.
[37] C.S. Klug, J.B. Feix, Methods and applications of site-directed spin labeling EPR spectroscopy, Methods Cell Biol. 84 (2008) 617–658.
[38] G. Paradies, V. Paradies, V. De Benedictis, F.M. Ruggiero, G. Petrosillo, Functional role of cardiolipin in mitochondrial bioenergetics, Biochim. Biophys. Acta 1837 (2014) 408–417.
[39] J. Planas-Iglesias, H. Dwarakanath, D. Mohammadyani, N. Yanamala, V.E. Kagan, J. Klein-Seetharaman, Cardiolipin interactions with proteins, Biophys. J. 109 (2015) 1282–1294.
[40] S.M. Claypool, Y. Oktay, P. Boontheung, J.A. Loo, C.M. Koehler, Cardiolipin defines the interactome of the major ADP/ATP carrier protein of the mitochondrial inner membrane, J. Cell Biol. 182 (2008) 937–950.
[41] U. Schlattner, M. Tokarska-Schlattner, S. Ramirez, A. Bruckner, L. Kay, C. Polge, R.F. Epand, R.M. Lee, M.L. Lacombe, R.M. Epand, Mitochondrial kinases and their molecular interaction with cardiolipin, Biochim. Biophys. Acta 1788 (2009) 2032–2047.
[42] R.P. Rand, S. Sengupta, Cardiolipin forms hexagonal structures with divalent cations, Biochim. Biophys. Acta 255 (1972) 484–492.
[43] B. Jolanta, B. Joanna, H.Z. Diana, S. Krystyna, Composition and concentration of serum fatty acids of phospholipids depend on tumour location and disease progression in colorectal patients, J Med Biochem 37 (2018) 39–45.
[44] M. Zhang, E. Mileykovskaya, W. Dowhan, Gluing the respiratory chain together. Cardiolipin is required for supercomplex formation in the inner mitochondrial membrane, J. Biol. Chem. 277 (2002) 43553–43556.
[45] P.L. Pedersen, J.W. Greenawalt, B. Reynafarje, J. Hullihen, G.L. Decker, J.W. Soper, E. Bustamente, Preparation and characterization of mitochondria and submitochondrial particles of rat liver and liver-derived tissues, Methods Cell Biol. 20 (1978) 411–481.
[46] A. Vogel, H.A. Scheidt, D. Huster, The distribution of lipid attached spin probes in bilayers: application to membrane protein topology, Biophys. J. 85 (2003) 1691–1701.
[47] D. Hockenbery, G. Nunez, C. Milliman, R.D. Schreiber, S.J. Korsmeyer, Bcl-2 is an inner mitochondrial membrane protein that blocks programmed cell death, Nature 348 (1990) 334–336.
[48] B. Schopf, H. Weissensteiner, G. Schafer, F. Fazzini, P. Charoentong, A. Naschberger, B. Rupp, L. Fendt, V. Bukur, I. Giese, P. Sorn, A.C. Sant'Anna-Silva, J. Iglesias-Gonzalez, U. Sahin, F. Kronenberg, E. Gnaiger, H. Klocker, OXPHOS remodeling in high-grade prostate cancer involves mtDNA mutations and increased succinate oxidation, Nat. Commun. 11 (2020) 1487.
[49] V. Kirkin, S. Joos, M. Zornig, The role of Bcl-2 family members in tumorigenesis, Biochim. Biophys. Acta 1644 (2004) 229–249.
[50] P.S. Ward, C.B. Thompson, Metabolic reprogramming: a cancer hallmark even Warburg did not anticipate, Cancer Cell 21 (2012) 297–308.
[51] R.A. Capaldi, Structure and function of cytochrome c oxidase, Annu. Rev. Biochem. 59 (1990) 569–596.
[52] P.C. Herrmann, J.W. Gillespie, L. Charboneau, V.E. Bichsel, C.P. Paweletz, V.S. Calvert, E.C. Kohn, M.R. Emmert-Buck, L.A. Liotta, E.F. Petricoin 3rd, Mitochondrial proteome: altered cytochrome c oxidase subunit levels in prostate cancer, Proteomics 3 (2003) 1801–1810.
[53] K. Zhang, Y. Chen, X. Huang, P. Qu, Q. Pan, L. Lu, S. Jiang, T. Ren, H. Su, Expression and clinical significance of cytochrome c oxidase subunit IV in colorectal cancer patients, Arch. Med. Sci. 12 (2016) 68–77.
[54] F.B. Mullauer, J.H. Kessler, J.P. Medema, Betulinic acid induces cytochrome c release and apoptosis in a Bax/Bak-independent, permeability transition pore dependent fashion, Apoptosis 14 (2009) 191–202.
[55] M. Flasinski, K. Hac-Wydro, M. Broniatowski, Incorporation of pentacyclic triterpenes into mitochondrial membrane—studies on the interactions in model 2D lipid systems, J. Phys. Chem. B 118 (2014) 12927–12937.
[56] N.C. Robinson, Functional binding of cardiolipin to cytochrome c oxidase, J. Bioenerg. Biomembr. 25 (1993) 153–163.
[57] P.R. van Ginkel, D. Sareen, L. Subramanian, Q. Walker, S.R. Darjatmoko, M.J. Lindstrom, A. Kulkarni, D.M. Albert, A.S. Polans, Resveratrol inhibits tumor growth of human neuroblastoma and mediates apoptosis by directly targeting mitochondria, Clin. Cancer Res. 13 (2007) 5162–5169.
[58] M.R. de Oliveira, S.F. Nabavi, A. Manayi, M. Daglia, Z. Hajheydari, S.M. Nabavi, Resveratrol and the mitochondria: from triggering the intrinsic apoptotic pathway to inducing mitochondrial biogenesis, a mechanistic view, Biochim. Biophys. Acta 1860 (2016) 727–745.
[59] S.E. Horvath, G. Daum, Lipids of mitochondria, Prog. Lipid Res. 52 (2013) 590–614.
[60] S. Raza Shaikh, D.A. Brown, Models of plasma membrane organization can be applied to mitochondrial membranes to target human health and disease with polyunsaturated fatty acids, Prostaglandins Leukot. Essent. Fat. Acids 88 (2013) 21–25.
[61] E. Zinser, C.D. Sperka-Gottlieb, E.V. Fasch, S.D. Kohlwein, F. Paltauf, G. Daum, Phospholipid synthesis and lipid composition of subcellular membranes in the unicellular eukaryote Saccharomyces cerevisiae, J. Bacteriol. 173 (1991) 2026–2034.
[62] A. Sorvina, C.A. Bader, C. Caporale, E.A. Carter, I.R.D. Johnson, E.J. Parkinson-Lawrence, P.V. Simpson, P.J. Wright, S. Stagni, P.A. Lay, M. Massi, D.A. Brooks, S.E. Plush, Lipid profiles of prostate cancer cells, Oncotarget 9 (2018) 35541–35552.
[63] L. Peyta, K. Jarnouen, M. Pinault, C. Guimaraes, J.P. Pais de Barros, S. Chevalier, J.F. Dumas, F. Maillot, G.M. Hatch, P. Loyer, S. Servais, Reduced cardiolipin content decreases respiratory chain capacities and increases ATP synthesis yield in the human HepaRG cells, Biochim. Biophys. Acta 1857 (2016) 443–453.
[64] M. Schlame, D. Rua, M.L. Greenberg, The biosynthesis and functional role of cardiolipin, Prog. Lipid Res. 39 (2000) 257–288.
[65] S.Y. Choi, F. Gonzalvez, G.M. Jenkins, C. Slomianny, D. Chretien, D. Arnoult, P.X. Petit, M.A. Frohman, Cardiolipin deficiency releases cytochrome c from the inner mitochondrial membrane and accelerates stimuli-elicited apoptosis, Cell Death Differ. 14 (2007) 597–606.
[66] T.A. Scott, R. Arnold, J.A. Petros, Mitochondrial cytochrome c oxidase subunit 1 sequence variation in prostate cancer, Scientifica (Cairo) 2012 (2012) 701810.
[67] A. Musatov, N.C. Robinson, Bound cardiolipin is essential for cytochrome c oxidase proton translocation, Biochimie 105 (2014) 159–164.
[68] S. Cogliati, J.A. Enriquez, L. Scorrano, Mitochondrial cristae: where beauty meets functionality, Trends Biochem. Sci. 41 (2016) 261–273.
[69] J. Fonseca, F. Moradi, L.A. Maddalena, B. Ferreira-Tollstadius, S. Selim, J.A. Stuart, Resveratrol integrates metabolic and growth effects in PC3 prostate cancer cells-involvement of prolyl hydroxylase and hypoxia inducible factor-1, Oncol. Lett. 17 (2019) 697–705.